CORA Cork Open Research Archive
Cartlann Taighde Oscailte Chorcaí

Title	Surface orientation effects in crystalline-amorphous silicon interfaces
Authors	Nolan, Michael;Legesse, Merid;Fagas, Gíorgos
Publication date	2012-09-25
Original Citation	Nolan, M., Legesse, M. and Fagas, G. (2012) 'Surface orientation effects in crystalline-amorphous silicon interfaces', Physical Chemistry Chemical Physics, 14(43), pp. 15173-15179. doi: 10.1039/C2CP42679J
Type of publication	Article (peer-reviewed)
Link to publisher's version	10.1039/C2CP42679J
Rights	© the Owner Societies 2012; Published by Royal Society of Chemistry. This is the Accepted Manuscript version of a published work that appeared in final form in Physical Chemistry Chemical Physics. To access the final published version of record, see http://pubs.rsc.org/en/content/articlepdf/2012/cp/c2cp42679j
Download date	2024-05-07 17:02:56
Item downloaded from	https://hdl.handle.net/10468/1604

UCC
University College Cork, Ireland
Coláiste na hOllscoile Corcaigh

Journal Name

Dynamic Article Links ►

Cite this: DOI: 10.1039/c0xx00000x

www.rsc.org/xxxxxx

ARTICLE TYPE

Surface Orientation Effects in Crystalline-Amorphous Silicon Interfaces

Michael Nolan*, Merid Legesse and Giorgos Fagas*

Received (in XXX, XXX) Xth XXXXXXXXX 200X, Accepted Xth XXXXXXXXX 200X
First published on the web Xth XXXXXXXXX 200X
DOI: 10.1039/

Abstract

In this paper we present the results of empirical potential and density functional theory (DFT) studies of models of interfaces between amorphous silicon (a-Si) or hydrogenated amorphous Si (a-Si:H) and crystalline Si (c-Si) on three unreconstructed silicon surfaces, namely (100), (110) and (111). In preparing models of a-Si on c-Si, melting simulations are run with classical MD at 3000 K for 10 ps to melt part of the crystalline surface and the structure is quenched to 300K using a quench rate of 6 x 10^{12} K/s and finally relaxed with DFT. Incorporating the optimum hydrogen content in a-Si to passivate undercoordinated Si, followed by DFT relaxation, produces hydrogenated amorphous silicon on crystalline surfaces, a-Si:H/c-Si. The (100) surface is the least stable crystalline surface and forms the thickest amorphous Si region, while the most stable (110) surface forms the smallest amorphous region. Calculated radial distribution functions (RDF) in the amorphous and crystalline layers are consistent with a-Si and c-Si and indicate a structural interface region one layer thick. The electronic density of states shows an evolution from c-Si to a-Si (or a-Si:H), with a larger electronic interface layer, suggesting that the electronic properties are more strongly perturbed by interface formation compared to the atomic structure. The computed optical absorption spectra show strong effects arising from the formation of different a-Si and a-Si:H regions in different Si surfaces.

1. Introduction

Heterojunctions of hydrogenated amorphous and crystalline silicon, henceforth denoted a-Si:H/c-Si, have gained much attention recently motivated by the so-called "Heterojunction with Intrinsic Thin layer (HIT)" solar cell[1]. This is because of demonstrated high efficiencies (above 23% on 100 cm^2 active area)[2]. In addition, from a technical point of view, the energy consumption and costly processing steps used to form the junctions or back surface field in the traditional crystalline solar cell fabrication are replaced with the low temperature processing steps of silicon thin film deposition. Currently most studies are devoted to a-Si:H/c-Si heterojunctions which are promising for solar applications because of better light absorption in the visible region compared to crystalline Si, widely used in solar cells. In order to advance the application of a-Si:H/c-Si in solar cell technology, further work is needed to understand the fundamental properties of this system and the interface between amorphous and crystalline Si.

a-Si:H/c-Si brings challenges in understanding factors such as surface orientation, the role of the interface region, the amount of hydrogen needed to passivate the dangling silicon and the influence of hydrogen in electronic and optical properties. A better understanding will improve a-Si:H/c-Si heterojunctions because these challenges influence device performance.

In this regard first principles simulations of model a-Si:H/c-Si interfaces can play an important role. There have been some experimental and theoretical studies of a-Si/c-Si and a-Si:H/c-Si interfaces, *e.g.* in refs. 3-8. But the inaccessibility of the interface atomic structure to experimental probes and the size of systems that can be handled by simulation and the extent of configuration space that can be explored through calculations have placed restrictions on understanding and improving the properties of a-Si:H/c-Si heterojunctions. Despite the importance of the a-Si:H/c-Si system, there has only been one recent first principles study of a model interface by Tosolini *et al.*[7]; these authors showed that the formation of the interface between a-Si:H and c-Si induces changes in the structural properties, but the electronic properties were not examined in detail.

In this paper, as part of our work on a-Si:H/c-Si interfaces for solar cell applications, we present results of first principles simulations of a-Si:H/c-Si interface models constructed from Si (110), (110) and (111) surfaces. These atomic-scale simulations of the interfaces are aimed at clarifying several

This journal is © The Royal Society of Chemistry [year]

questions concerning the structural and electronic and optical properties of a-Si:H/c-Si heterojunctions and any dependence on the Si surface orientation and interface structure. We present herein an initial study of a-Si:H/c-Si interfaces in which aSi is formed from partially melted and quenched models of the (100), (110) and (111) Si surfaces. Our results show that surface orientation can play a key role in the interface and electronic and optical properties in a-Si:H/c-Si. In addition, we also find that two interfaces can be identified, a structural interface that extends over a single atomic layer and an electronic interface that extends over 3-4 atomic layers.

2. Methodology

We apply a heat and quench approach to generate models of a-Si:H/c-Si, starting from unreconstructed, bulk terminated crystalline Si (100), (110) and (111) surfaces, using the classical molecular dynamics code GULP[9]. The surfaces are (2 x 2) surface supercells and are bulk cleaved to have 512 atoms in (100) and (111) (32 layers) and 522 atoms in (110) (29 layers) to minimise the influence of the size of the surface model on formation of the amorphous region. Within a molecular dynamics framework, heat and quench is a very common approach for generating models of amorphous silicon. The Tersoff interatomic potential is used for Si[10], with the cut-offs set as 2.7 Å (Taper) and 3.0 Å (Maximum)[10]; this potential has been used extensively for c-Si and a-Si[11, 12]. In the two dimensional periodic boundary condition MD simulations we run an initial "melting" simulation at 3000 K for 10 ps in the constant volume and temperature ensemble (NVT), using a simulation timestep of 0.1 fs. This 10 ps simulation allows for some melting of the initially crystalline Si surface, while the extent of melting in the surface will depend on the surface stability (Sec. 3.1); in subsequent work we are examining formation of different relative thicknesses of a-Si:H and c-Si in each surface by running melting simulations with different total simulation times. The structure resulting from the 10 ps simulation is subsequently quenched to 300 K using a cooling rate of $6x10^{12}$ K/s. This cooling rate is consistent with the literature data, e.g. refs. 13 - 15, where cooling rates between 10^{11} and 10^{15} K/s have been used. Our cooling rate falls within this range and allows us to obtain a disordered a-Si region interfaced with a crystalline region after quenching from the melt. After quenching, the a-Si-c-Si interfaces are annealed for 25 ps at 300 K. We have run 5 individual heat and quench simulations under the above conditions and have found that the extent of the disordered region in each surface is the same in each run, so that our results can be considered a robust representation of the amorphous-crystalline interface in each surface orientation. For each surface, we selected one quenched structure to be further investigated.

All structural, electronic and optical properties of the heterostructures are calculated from structures determined from ionic relaxations using density functional theory (DFT)[16] implemented in the VASP5.2 code[17]. We use the generalized gradient approximation of Perdew-Burke-Ernzerhof, PBE-GGA,[18] to the exchange-correlation functional. The interaction between ion cores and valence electrons are described using the projector-augmented wave method (PAW)[19], with 4 electrons on Si and 1 electron on H. The electronic wavefunctions are described within a plane wave basis set and the kinetic-energy cut-off is set to 400 eV. Irreducible Brillouin zone integration for all surface supercells is conducted using Γ point sampling[20]. A Gaussian smearing of width 0.1 eV is applied to determine the band occupations and electronic density of states.

By incorporating hydrogen into the a-Si region to passivate all undercoordinated Si in each surface supercell, we generate interface models of a-Si:H/c-Si in (100), (110) and (111), with optimum hydrogen concentrations of 40, 16 and 28 hydrogen atoms (17%, 14% and 18%, in the amorphous regions) respectively. These saturated models structures of a-Si:H/c-Si are relaxed with GGA-DFT. Concerning the use of GGA-DFT for modelling the electronic properties of a-Si, we have studied the interplay of structure and function in bulk a-Si and a-Si:H with this heat and quench approach and PBE-GGA. Our results for a-Si/a-Si:H are in good qualitative agreement with experiment and results from hybrid DFT back up our major findings with PBE-GGA, giving confidence in using PBE-GGA for a-Si.

3. Results

3.1 Atomic structure of a-Si-c-Si interface models

Figures 1-3 show the atomic structure of the relaxed non-hydrogenated a-Si/c-Si and the relaxed hydrogenated a-Si:H/c-Si models for the (100), (110) and (111) Si surfaces. Experimental and theoretical surface energy calculations [21-23] indicate that of the bulk terminated unreconstructed surfaces considered in this work, the stability is as follows: (100) < (111) < (110). Upon examining the structures generated from the initial 10 ps melt simulation, the (100) surface has the largest amorphous region, with the most stable (110) surface displaying the smallest amorphous region. This is consistent with the stability of each surface found from the surface energies and suggests that the orientation of the Si surface can play a role in determining the relative thickness of an a-Si layer on c-Si.

In figures 1-3, the Si-Si radial distribution function (RDF) is shown in a layer-by-layer format in selected crystalline and amorphous layers, where a layer is defined as a region that is half the Si lattice constant; the supplementary information shows the RDF for all layers in the structures. The RDF measures the local structure in a-Si and is experimentally accessible, providing a useful tool for comparing the computationally created structures with real samples. In crystalline materials, there are sharp peaks at the neighbouring, next neighbour etc Si-Si distances, indicative of short and long range order. In amorphous Si, while there is a peak at the nearest neighbour Si-Si distance, indicating short range order, the disorder present means that the RDF peaks are broadened and coalesce, indicative of no long range order. In figures 1-3, both the crystalline and amorphous regions

This journal is © The Royal Society of Chemistry [year]

show RDFs that are typical of bulk crystalline and amorphous Si[21], with the aSi layers showing no defined peaks indicating no long range order.

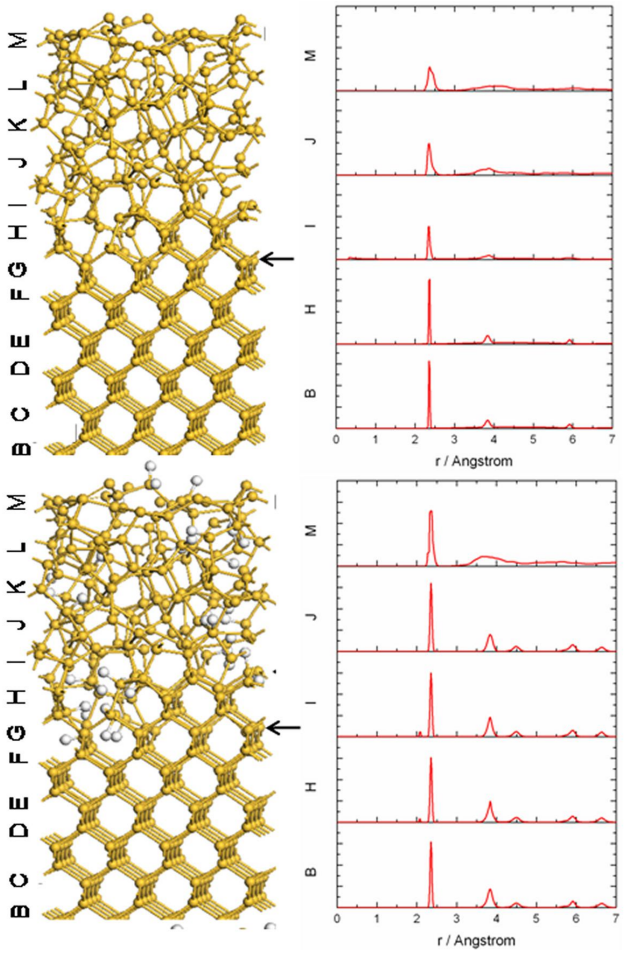

Fig. 1 Atomic structure and layer resolved radial distribution function of a-Si/c-Si and a-Si:H/c-Si interface models in the (100) Si surface. The labelling of the layers runs from B (crystalline) to M (amorphous). Si atoms are yellow spheres and H atoms are white. The black arrow indicates the interface region.

The apparent amorphous regions (layers I – M in (100), figure 1; layer M in (110), figure 2; layers L – M in (111), figure 3) show a defined peak at the neighbouring Si-Si distance, with a reduced maximum and increased broadening in this peak compared with the crystalline RDF. The second and subsequent peaks are typical of amorphous Si.

Examining the RDF, we can also attempt to identify an interface region, which we term the structural interface. For (100), this can be considered to be in layer G, where it is clear that Si atoms are displaced from their lattice sites, when compared to layer B for example. For the (110) surface it is layer L and for (111) it is layer J. In these layers, while the RDF is obviously not characteristic of an amorphous region it nonetheless is also not typical of crystalline Si and it is clear that the peak heights are reduced and the peak widths are bigger, indicating that the interface region is intermediate between c-Si and a-Si and we find this interface to be one layer thick.

We have determined the number of undercoordinated (2 and 3-fold) and 5 coordinated Si in the a-Si region of the heterostructures. For (100), 11% of Si are not 4-fold coordinated, while in the (110) and (111) surfaces, 5 % and 8 % of Si atoms are not 4-fold coordinated. Interestingly, the total density of dangling and floating defects follows the inverse order to the surface stability of the various orientations (100) > (111) > (110).

We have added hydrogen (as discussed in section 2) to passivate the dangling Si bonds in the a-Si layer and relax these a-Si:H/c-Si interfaces with DFT. Figure 2 shows the atomic structure of the relaxed a-Si:H/c-Si interfaces for the (100), (110) and (111) surfaces as well as the layer resolved RDF. On computing the Si coordination numbers, we find that the number of Si atoms that are not 4-fold coordinated are reduced to 1.4 %, 0.5 % and 1% in (100), (110) and (111), yielding again higher density of coordination defects for the surfaces with lower stability.

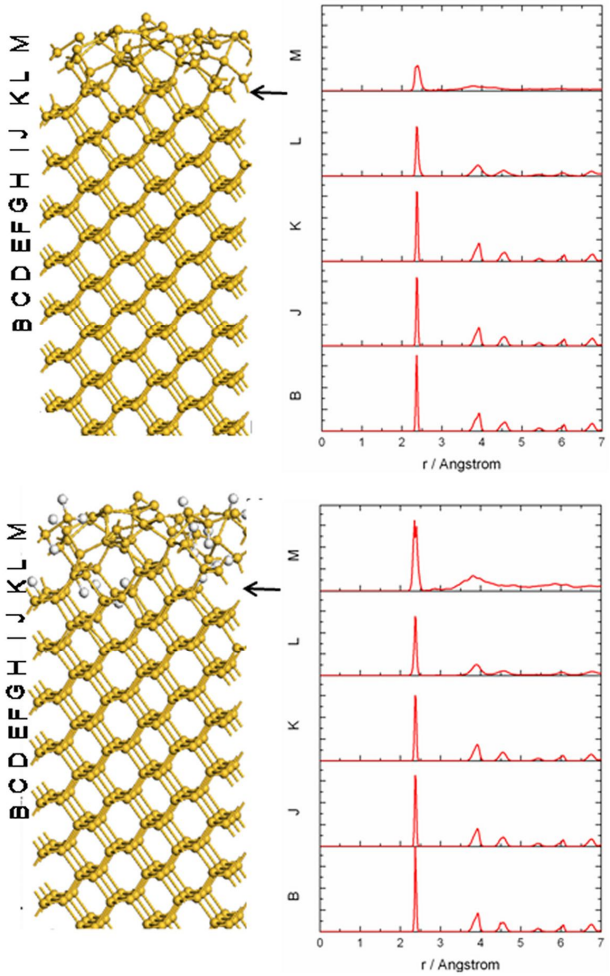

Fig. 2 Atomic structure and layer resolved radial distribution function of a-Si/c-Si and a-Si:H/c-Si interface models in the (110) Si surface. The labelling of the layers runs from B (crystalline) to M (amorphous). Si atoms are yellow spheres and H atoms are white. The black arrow indicates the interface region.

The RDF for the a-Si:H/c-Si interface in the (100) surface can be compared with that of the non-hydrogenated surface (see fig. 1) and we find that the presence of hydrogen improves the

This journal is © The Royal Society of Chemistry [year]

order in the non-crystalline layers, as indicated by the coordination numbers, but the RDF of the interface region remains consistent with an amorphous structure. For the other surfaces, the inclusion of hydrogen also improves the order in the interface region. For example, for the (110) surface the presence of hydrogen leads to higher values of the first and second maximum of the RDF *of layer L* compared with the non-hydrogenated structures in fig 2. The reason for this is that including hydrogen increases the number of four-fold Si in the structure and therefore reduces the number of undercoordinated Si and strained Si-Si bonds. Finally, in the (111) surface, layer J is the interface layer, with an increase in short and medium range order, as indicated by the first two peaks in the RDF (fig. 3).

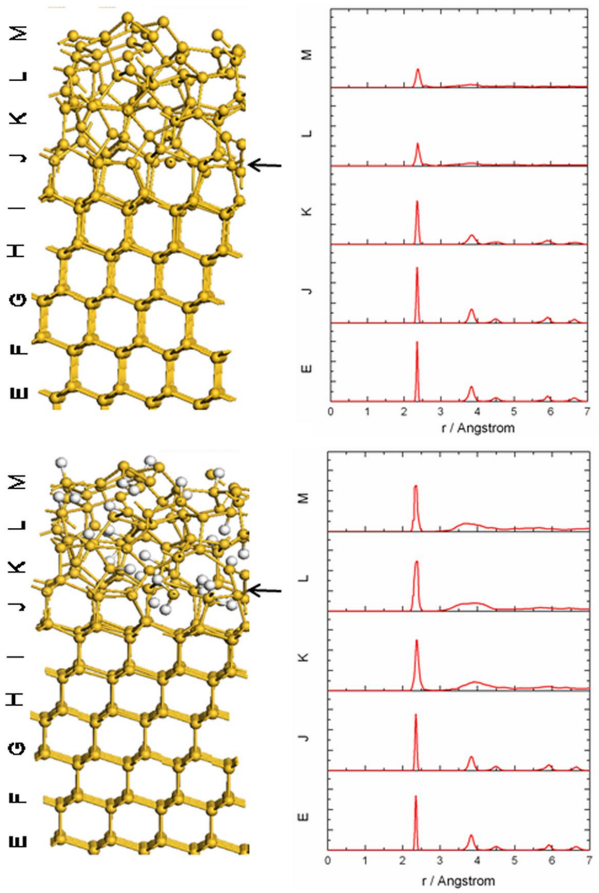

Fig. 3 Atomic structure and layer resolved radial distribution function of a-Si/c-Si and a-Si:H/c-Si interface models in the (111) Si surface. The labelling of the layers runs from E (crystalline) to M (amorphous). Si atoms are yellow spheres and H atoms are white. The black arrow indicates the interface region.

3.2 Electronic Properties of a-Si:H/c-Si interfaces

a-Si:H and c-Si display different electronic properties as a result of their different structures. c-Si shows a clear valence band to conduction band energy gap and no states in the energy gap. a-Si:H shows the well known tail states and a larger energy gap than c-Si, which arises from the disorder present in a-Si:H[24-26]. Amorphous Si is characterised by the valence and conduction band mobility edges and the presence of electronic states around the Fermi level, arising from the presence of undercoordinated Si, which are removed by incorporation of hydrogen.

To examine the electronic properties in the interface models, we show in figures 4 and 5 the total electronic density of states (EDOS) in the crystalline Si layers nearest the interface (not all c-Si layers are shown, since the EDOS is unchanged in the layers farthest away from the interface) through the interface and in the a-Si or a-Si:H layers in a 2-D stacked plot. Figure 4 shows the layer-by-layer EDOS in the non-hydrogenated a-Si/c-Si surfaces and figure 5 shows the EDOS in the hydrogenated a-Si:H/c-Si surfaces; the SI displays the EDOS for all layers of the heterostructures.

For the c-Si region, the EDOS shows a clear separation between the valence and conduction bands. When we go from crystalline region to amorphous there is a change in the nature of the EDOS. Taking first non-hydrogenated a-Si/c-Si interfaces, we see that in the (100) surface, regions G and H already start to show a deviation from the c-Si EDOS to an EDOS characterised by formation of valence and conduction band tails, signifying the onset of disorder in these layers. By region I, a clear signature of a-Si in the EDOS is present, namely in-gap states due to undercoordinated Si and the band tails. In the a-Si regions in each surface, the DOS is non-vanishing at the Fermi energy. This originates from the characteristics of amorphous Si, primarily attributed to the existence of structural defects which arise from dangling bonds and long Si-Si (strained) bonds[24-26]. Taken in general, the EDOS in the amorphous regions has the typical form of bulk a-Si and the EDOS in the crystalline regions is typical of bulk c-Si.

For the (110) and (111) surfaces, the EDOS shows that the amorphous region extends over fewer layers compared to the (100) surface, consistent with the structural analysis. In the (110) and (111) surfaces, we see that in layers I the EDOS is modified from that of c-Si and in region L and J, which were identified as the structural interface layer, the EDOS shows amorphous character.

In the hydrogenated a-Si:H-c-Si interfaces, the crystalline regions have a EDOS consistent with c-Si. Taking the (100) surface, with the largest amorphous region, regions G – J, display a DOS that is consistent with less disorder in these layers compared to the non-hydrogenated interface as a result of hydrogen incorporation. This is characterised by the removal of the states around the Fermi level, with the band tails persisting. Regions K – M therefore display an EDOS consistent with bulk hydrogenated a-Si with an optimum hydrogen concentration that removes the defect-induced electronic states around the Fermi level. In the (110) and (111) surfaces, we find a similar change in the electronic properties as a result of hydrogen incorporation.

It is interesting to contrast the identification of any interface between the amorphous and crystalline regions from the structural and electronic information in our model a-Si/c-Si heterostructures. Using the RDF (structural), the interface between the two regions appears to be abrupt, being essentially over one layer. However, the EDOS would indicate that the interface region is spread over a larger region, with

This journal is © The Royal Society of Chemistry [year]

characteristics of disorder appearing in layers that display an RDF characteristic of crystalline silicon. On examining the structures, we can see that the layers displaying a modified EDOS (compared to c-Si) show Si atoms displaced off their lattice sites, but not to the extent seen in the a-Si and a-Si:H layers. However, the RDF in these layers is little changed from the c-Si layers and is less sensitive to small changes in the local atomic structure when compared to the EDOS. We suggest that an interface region can be best identified from analysis of the electronic density of states.

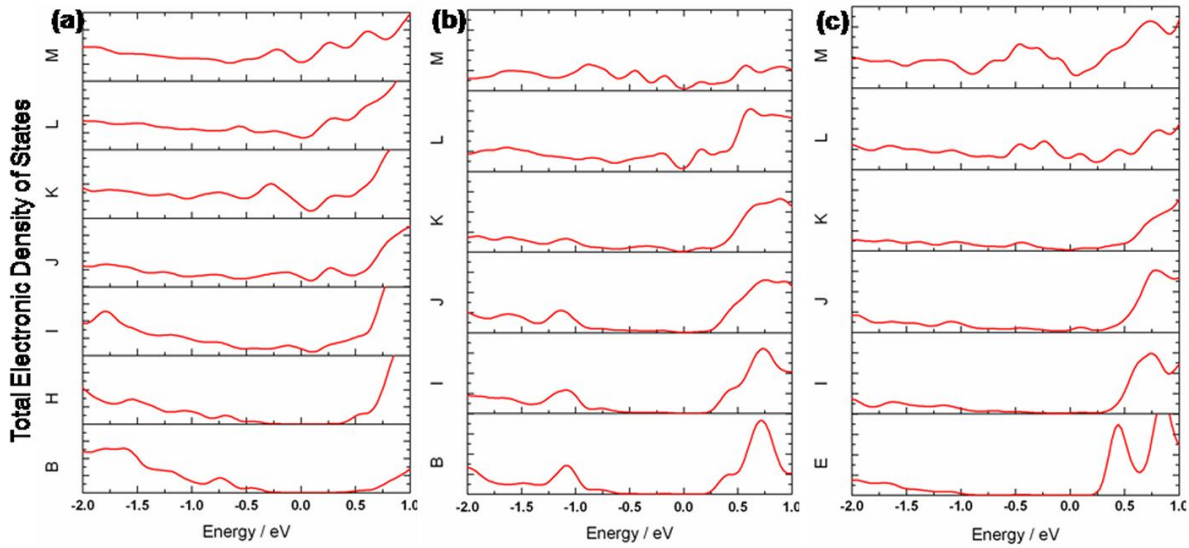

Fig. 4 Layered-resolved total electronic density of states (EDOS) plots for each unhydrogenated interface structure. **(a):** (100) surface, **(b):** (110) surface, **(c):** (111) surface. The EDOS for selected crystalline layers are shown (bottom plot), since the EDOS are invariant on going through the crystalline layers. The zero of energy is referenced to the Fermi level determined with VASP for the individual structures and we display valence band states to 2 eV below the Fermi level and conduction band states to 1 eV above the Fermi level.

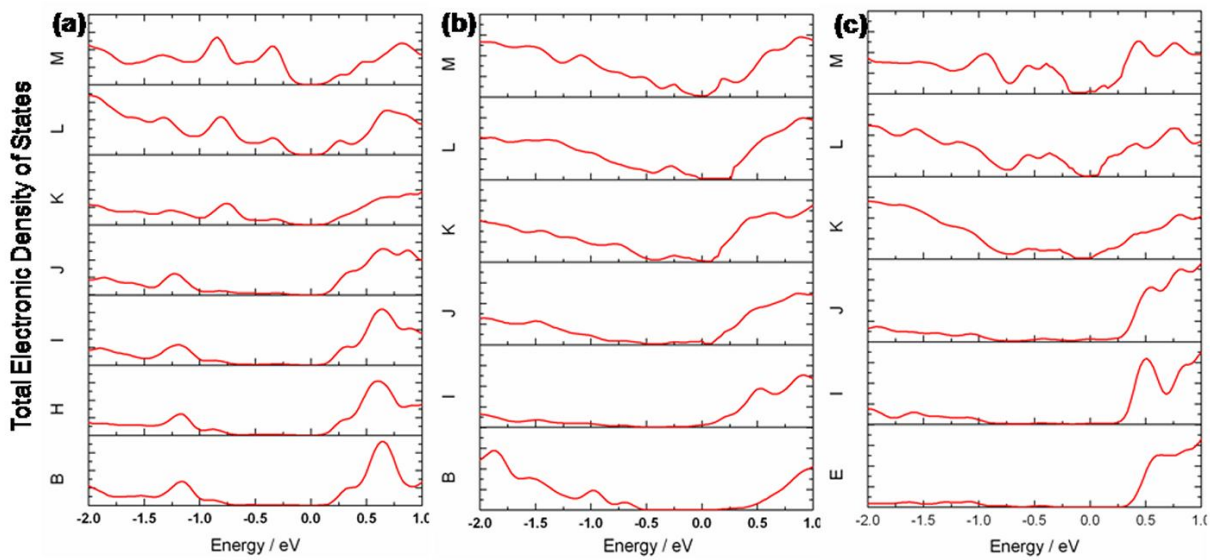

Fig. 5 Layered-resolved total electronic density of states (EDOS) plots for each hydrogenated interface structure. **(a):** (100) surface, **(b):** (110) surface, **(c):** (111) surface. The EDOS for selected crystalline layers are shown (bottom plot), since the EDOS are invariant on going through the crystalline layers. The zero of energy is referenced to the Fermi level determined with VASP for the individual structures and we display valence band states to 2 eV below the Fermi level and conduction band states to 1 eV above the Fermi level.

This journal is © The Royal Society of Chemistry [year]

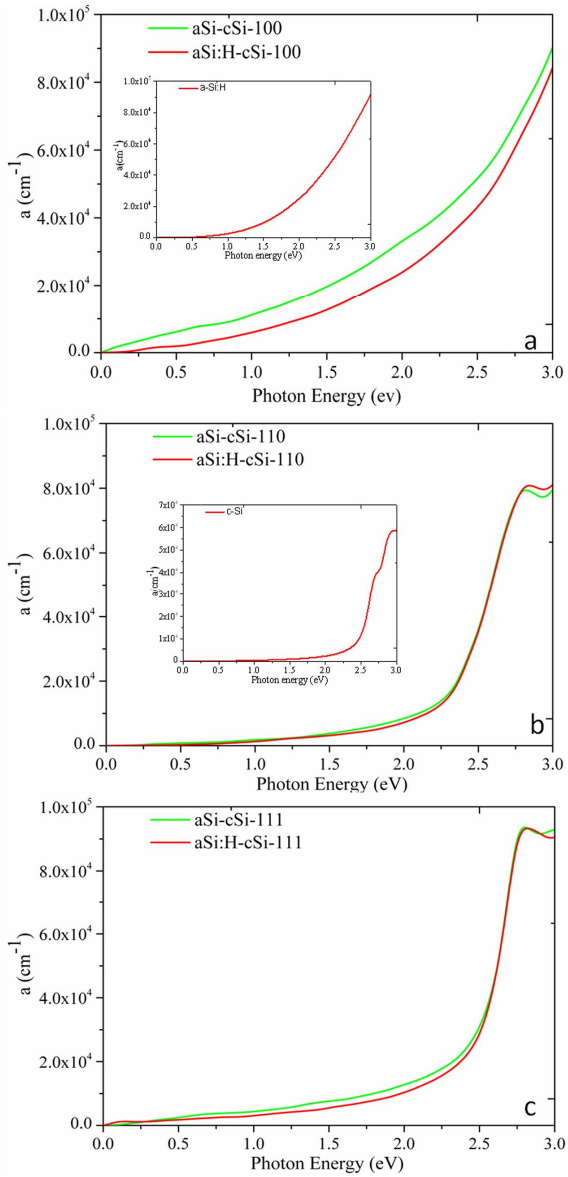

Fig.6. Computed optical absorption spectra for the a-Si/c-Si and a-Si:H/c-Si interface models. **(a)**: (100), **(b):** (110) and **(c):** (111). The insets show the optical absorption spectra for bulk a-Si:H and bulk c-Si

The optical absorption spectrum has been calculated for each of the a-Si:H/c-Si interfaces and these are shown in figure 6. The real and imaginary parts of the dielectric function are computed using the routines of Furthmuller[27] and the absorption coefficient is calculated from

$$\alpha = 2\kappa\pi/\lambda \quad (1)$$

Where λ is the free space wavelength of light, κ is the extinction coefficient, calculated from:

$$\kappa = 1/\sqrt{2}\ (-\varepsilon_1 + (\varepsilon_1^2 + \varepsilon_2^2)) \quad (2)$$

and ε_1 and ε_2 are the real and imaginary parts of the dielectric function. Also shown in figure 6 are the optical absorption spectra for bulk c-Si and bulk a-Si:H. For c-Si, only direct gap absorption can be treated in this formalism.

On comparing firstly the bulk spectra to those of the interface models, we find that the spectrum of (100) interface is dominated by absorption in the a-Si and a-Si:H regions, being similar to that of bulk a-Si and a-Si:H. In contrast, the (110) and (111) interfaces have an optical absorption spectrum similar to crystalline silicon, so that with thinner amorphous regions, the optical absorption is dominated by the crystalline region. On closer examination, we see that the (110) interface shows an onset of absorption at larger energy than the (111) surface, which is consistent with the (110) interface having the smallest amorphous region. At the same time, the presence of the amorphous region in the (110) interface leads a lower energy absorption onset compared with pure c-Si, so that the amorphous region, even if small, can affect the optical properties.

4. Conclusions

In this work, interface models of amorphous-crystalline silicon are generated in Si (100), (110) and (111) surfaces. The interface models are characterised by structure, radial distribution function, electronic density of states and optical absorption spectrum. We find that the least stable (100) surface will result in the formation of the thickest amorphous silicon layer with the highest density of coordination defects, while the most stable (110) surface forms the smallest amorphous region with the least defects. Analysis of the RDF indicates a **structural interface region** one layer thick in both a-Si/c-Si and a-Si:H/c-Si interface. In a-Si/c-Si, the electronic density of states shows new electronic states forming as a result of disorder, even in the seemingly crystalline layers, since the EDOS is more sensitive to small perturbations in the atomic positions from their perfect lattice sites than is the RDF, so that the use of the RDF alone to identify an interface region is not sufficient. The a-Si layers show a DOS typical of bulk a-Si. Addition of hydrogen to the a-Si region changes the DOS in a similar fashion to bulk a-Si, due to passivation of dangling silicon atoms. Finally computed optical absorption spectra demonstrate that for thick amorphous layers, the optical absorption is dominated by a-Si, while thinner layers show an optical absorption spectrum characteristic of crystalline silicon, but modified by the presence of the a-Si layer and this is driven by the stability of the crystalline Si surfaces. These results provide a useful starting point to further analyse the properties of a-Si/c-Si heterostructures prepared with different thicknesses of amorphous silicon, which is important for understanding and optimising the light absorption and charge dynamics of a-Si/c-Si solar cell heterostructures.

Acknowledgements

We acknowledge support from The European Commission, through the 7th Framework ICT-FET-Proactive program, Project: SiNAPS (contract no 257856). We also acknowledge

This journal is © The Royal Society of Chemistry [year]

computing resources provided by SFI to the Tyndall National Institute and by the SFI and Higher Education Authority Funded Irish Centre for High End Computing.

Notes and references

Tyndall National Institute, University College Cork, Lee Maltings, Cork, Ireland
E-mail: michael.nolan@tyndall.ie, georgios.fagas@tyndall.ie

1. M. Tanaka, M. Taguchi, T. Matsuyama, T. Sawada, S. Tsuda, S. Nakano, H. Hanafusa and Y. Kuwano, *Jpn. J. Appl. Phys., Part 1* 1992, **31**, 3518
2. Y. Tsunomura, Y. Yoshimine, M. Taguchi, T. Baba, T. Kinoshita, H. Kanno, H. Sakata, E. Maruyama and M. Tanaka, *Sol. Energy Mater. Sol.Cells* 2009, **93**, 670
3. H. Angermann, L. Korte, J. Rappich, E. Conrad, I. Sieber, M. Schmidt, K. Hübener and J. Hauschild, *Thin Solid Films* 2008, **516,** 6775
4. G. H. Gilmer and C. Roland, *Appl. Phys. Lett.,* 1994, **65**, 824
5. M. J. Caturla, T. D. de la Rubia and G. H. Gilmer, *J. Appl. Phys.* 1995, **77**, 3121
6. A. Descoeudres, L. Barraud, S. De Wolf, B. Strahm, D. Lachenal, C. Guerin, Z. C. Holman, F. Zicarelli, B. Demaurex, J. Seif, J. Holovsky and C. Ballif, *Appl. Phys. Lett.* 201, **97**, 183505
7. M. Tosolini, L. Colombo and M. Peressi, *Phys. Rev. B* 2004, **69**, 075301
8. M. Schmidt, L. Korte, A. Laades, R. Stangl, Ch. Schubert, H. Angermann, E. Conrad and K. V. Maydell, *Thin Solid Films* 2007, **515,** 7475
9. J. D. Gale and A. L. Rohl, *Molecular Simulation,* 2003, **29**, 291
10. J. Tersoff, *Phys. Rev. B* 1989, **39**, 5566; J. Tersoff, *Phys. Rev. Lett.,* 1989, **39**, 5566.
11. C. Krzeminski, Q. Brulin, V. Cuny, E. Lecat, E. Lampin and F. Cleri, *Appl. Phys. Lett.,* 2007, **101**, 123506
12. S. Izumi, S. Hara, T. Kumagai and S. Sakai, *Comp. Mater. Sci.* 2004, **31,** 256
13. M. Ishimaru, S. Munetoh and T. Motooka, *Phys Rev B* 1997, **56**, 15133,
14. I. Stich, R. Car and M. Parrinello, *Phys. Rev. B* 1991, **44**, 11094
15. K. Jarolimek, R. A. de Groot, G. A. de Wijs and M. Zeman, *Phys Rev B* 2009, **79**, 155206
16. W. Kohn and L.J. Sham, *Phys. Rev.* 1965, **A140**, 1133
17. G. Kresse and J. Furthmüller, *Phys. Rev. B* 1996, **54**, 11169
18. G. Kresse and D. Joubert, *Phys. Rev. B* 1999, **59**, 1758
19. J.P. Perdew, K. Burke and M. Ernzerhof, *Phys, Rev. Lett.* 1996, **77**, 3865
20. H. J. Monkhorst and J. D. Pack, *Phys. Rev. B*, 1976, **13**, 5188
21. A. A. Stekolnikov, J. Furthmu¨ller and F. Bechstedt, *Phys. Rev. B*, 2002, **65** 115318
22. A. A. Stekolnikov, J. Furthmu¨ller and F. Bechstedt, *Phys. Rev. B*, 2003, **67** 195332.
23. G-H. Lu, M. Huang, M. Cuma and F. Liu, *Surf. Sci* 2005, **588**, 61
24. Aljishi, J. D. Cohen, S. Jin, and L. Ley, *Phys. Rev. Lett*., 1990, 64, 2811.
25. Y. Pan, F. Inam, M. Zhang, and D.A D rabold, *Phys. Rev. Lett*., 2008, **100**, 206403.
26. P. A. Khomyakov, W. Andreoni, N. D. Afify and A. Curioni, *Phys. Rev. Lett,* 2011, **107**, 255502.
27. http://www.freeware.vasp.de/VASP/optics

Graphical Abstract

In amorphous-crystalline Si heterojunction interfaces, surface orientation plays important role in the thickness of the amorphous layer and the resulting structural electrical and optical properties.

 This journal is © The Royal Society of Chemistry [year]